Observer Based Current Estimation for Coupled Neurons

KLAUS RÖBENACK, NICOLAS DINGELDEY
Technische Universität Dresden
Institute of Control Theory
Faculty of Electrical and Computer Engineering
01062 Dresden
GERMANY
klaus.roebenack@tu-dresden.de

Abstract: The input current stimulating a neuron is not directly measurable without inference with the cell's activities. In this paper we consider two electrically coupled neurons. We present an approach to reconstruct the input current into one of the neurons using concepts from control theory. More precisely, we employ an unknown input observer to reconstruct the internal states of the neuron's model. A crucial part of this approach is the transformation of the nonlinear model into an appropriate normal form. Additional filtering yields the desired excitation current.

Key–Words: Hodgkin-Huxley model, Coupled neurons, Filter, Observer, Relative degree, Derivative estimation

1 Introduction

The development of an electro-physiological model of a neuron, published in 1952 by Hodgkin and Huxley, was a milestone in neuroscience. Some authors simplified the Hodgkin-Huxley model [12, 29] for analog as well as fast digital simulations, where other authors extended it in order to obtain a more realistic modeling [8, 48, 49]. Even sixty years after its publication, the Hodgkin-Huxley model is still widely used in computational neuroscience [43].

In living organisms, neurons are connected to each other in a complex fashion. As a first step to understand networked neurons, several researchers investigated the dynamics of two interconnected neurons [32, 34, 42, 48]. In particular, the problem of synchronization of two neurons draw significant attention [21, 46].

The stimulation of a neuron from another neuron is transmitted via ionic currents. The standard technique to measure ionic currents across the cell's membrane is known as voltage clamping [11]. This approach was developed in [7] and has been extended in [30]. Unfortunately, these approaches interfere with the cell's activity, limiting the applicability in vivo.

In control theory, the problem of reconstruction of not directly measurable quantities using the dynamics of the underlying system is known as filter or observer design [19, 23]. Starting with linear time-invariant systems, this work has been extended into several directions such as filter or observer design for time-varying and nonlinear systems [22, 25, 31, 35, 36, 41, 45, 51, 52], or the design of unknown input observers [4, 9, 16, 26].

For bio-systems, estimators based on observers or filters are also known as software sensors or software analyzers [3, 50]. Observer and filter technqiues can be used to reconstruct the input current into a single neuron using voltage measurement [37–39]. In this paper we want to extend these approaches to the case of two electrically coupled neurons.

This paper is structured as follows: In Section 2 we remind the reader of the Hodgkin-Huxley model. Moreover, we discuss possible scenarios for the coupling of two neurons. The required concepts from control theory are introduced in Section 3. Approaches to the observer based current estimation are explained in Section 4. Finally, we draw some conclusions in Section 5.

2 Neuron Models

2.1 Hodgkin-Huxley Model

The Hodgkin-Huxley model is a set of nonlinear ordinary differential equations (ODEs) describing the mechanisms of the initiation and propagation of action potentials in the squid giant axon [15]. It is a widely used standard model of neurons. More advanced neuron models such as the Connor-Steven model [8] or the Traub model [48] still use the same concept of modeling. Furthermore, this kind of modeling has also been extended to other cell and issue types such as muscle fibers [28], or pancreatic beta cells [6].

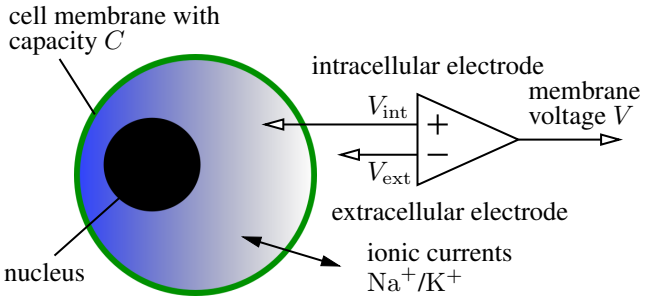

Figure 1: Measurement scheme for the membrane voltage

The Hodgkin-Huxley model describes the electro-physiological behaviour of a neuron. An important quantity of this model is the membrane voltage V, which is defined as the difference between potentials of the intracellular and extracellular medium. The measurement of the membrane voltage is sketched in Fig. 1. The cell's membrane acts mainly as an insulator having the capacitance C. However, the membrane acts also as a conductor. Let I be the current injected into the cell, e.g. by an electrode or from coupling with other cells. The Hodgkin-Huxley model takes also ionic currents into account. Let I_{Na} and I_K denote the currents resulting from sodium ions (Na^+) and potassium ions (K^+) passing through the cell's membrane. Additionally, the model contains a leak current I_L accounting for the natural permeability of the membrane. The principle of conservation of electric charge (Krichhoff's first law) yields the ODE

$$C\dot{V} = I - L_{Na} - I_K - I_L. \tag{1}$$

The ionic currents I_{Na}, I_K, and the leak current I_L are given by

$$\begin{aligned} I_{Na} &= g_{Na} m^3 h (V - V_{Na}) \\ I_K &= g_K n^4 (V - V_K) \\ I_L &= g_L (V - V_L) \end{aligned} \tag{2}$$

with constant conductances g_{Na}, g_K, g_L and the reversal potentials V_{Na}, V_K, V_L. The reversal potential of an ion is the membrane potential at which there is on average no flow of that ion from one side of the membrane to the other.

An important part of the Hodgkin-Huxley model is the introduction of ion channels. More precisely, the model consists of three ion channels. The channel describing the leak current has an constant conductance g_L. The other ionic currents are described by voltage-gated ion channels with the gating variables m, h, n. The Na^+ channel is gated in a combined fashion by the variables m and h, whereas the K^+ channel is controlled by the gating variable n, see Eq. (2). The dynamics of the gating variables is described by a Markov model as a set of nonlinear ODEs

$$\begin{aligned} \dot{m} &= \alpha_m(V)(1-m) - \beta_m(V) m \\ \dot{h} &= \alpha_h(V)(1-h) - \beta_h(V) h \\ \dot{n} &= \alpha_n(V)(1-n) - \beta_n(V) n \end{aligned} \tag{3}$$

with the normalized functions

$$\begin{aligned} \alpha_m(V) &= \tfrac{0.1(V+40)}{1-\exp(-(V+40)/10)} \\ \beta_m(V) &= 4\exp(-(V+65)/18) \\ \alpha_h(V) &= 0.07\exp(-V+65)/20 \\ \beta_h(V) &= \tfrac{1}{1+\exp(-(V+35)/10)} \\ \alpha_n(V) &= \tfrac{0.01(V+55)}{1-\exp(-(V+55)/10)} \\ \beta_n(V) &= 0.125\exp(-(V+65)/80). \end{aligned} \tag{4}$$

The gating variables are dimensionless since they describe the probability for the appropriate gate to be open. Therefore, they take values between 0 and 1, where 0 means that the gate is closed, and 1 means that the gate is open. The functions in (4) are transition rates for the opening and closing of the gate, respectively. They have been determined empirically by Hodgkin and Huxley [15].

The simulation result for a single neuron based on the Hodgkin-Huxley model is shown in Fig. 2. We used the parameters $C_m = 1\ \frac{\mu F}{cm^2}$, $g_{Na} = 120\ \frac{mS}{cm^2}$, $V_{Na} = 115\ mV$, $g_K = 36\ \frac{mS}{cm^2}$, $V_K = -12\ mV$, $g_L = 0.3\ \frac{mS}{cm^2}$ as found in [15]. Furthermore, we used the initial values $V_m(0) = 0mV$, $h(0) = 0.5961$ und $m(0) = 0.0529$, $n(0) = 0.3177$. The model (1)-(4) was stimulated by a time-dependent (but piecewise constant) input current I shown in the top of Fig. 2. For $I = 10\mu A/cm^2$ and $I = 30\mu A/cm^2$ the model generates periodic spikes. This regular spiking occurs for $I \gtrapprox 6\mu A/cm^2$. More details on the excitability and the dynamics of neurons can found in [20, 34].

2.2 Coupled Neurons

The dynamical behaviour of coupled neurons is regarded as highly interesting from the viewpoint of neuroscience. The coupling of neurons allows the transmission of stimuli, where the excitation of one neuron is inducted by an other neuron via a synapse. There are two forms of synaptic coupling found in living organisms [42], namely chemical and electrical coupling.

Chemical synaptic coupling of neurons is often described by highly complex models. To allow the analysis and simulation of a large collection of networked or coupled neurons, simpler models have been

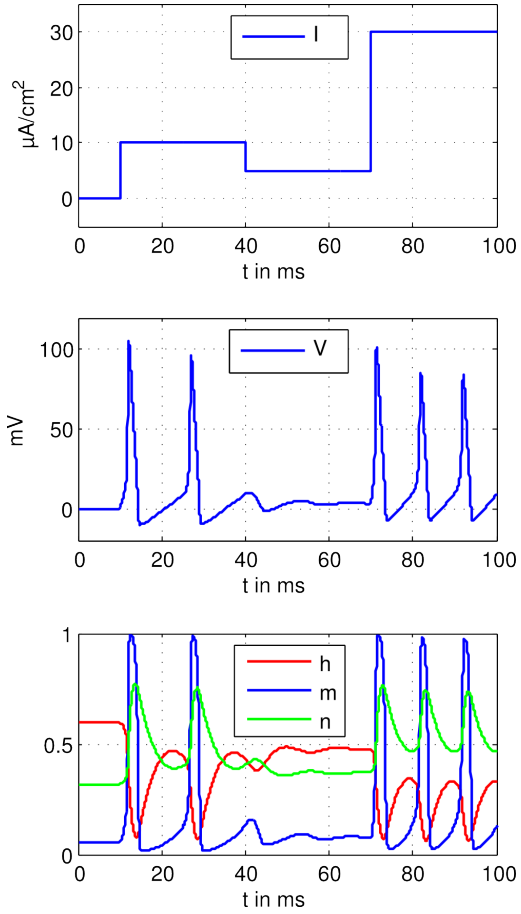

Figure 2: Simulation of a single neuron stimulated by a piece-wise constant input current I

derived. However, even very simple models should contain at least a lag element to describe the delay of the transmission, resulting in one or more differential equations [1, pp. 393-395].

In contrast to chemical coupling, the electrical synaptic coupling is essentially undelayed. In terms of an equivalent network description, electrical coupling between two neurons can be modeled by a resistors connecting the two membrane voltages V_1 and V_2, see [1, p. 393]. The resulting coupling current I_C is given by

$$I_C = g_C(V_1 - V_2), \tag{5}$$

where g_C is the conductance of the coupling resistor.

In this paper we consider two electrically coupled neurons. More precisely, two Hodgkin-Huxley models are interconnected by linear terms (5) in the first equations (1), that is

$$\begin{aligned} C_1\dot{V}_1 &= I_1 - g_{Na,1}m_1^3h_1(V_1 - V_{Na}) \\ &\quad -g_{K,1}n_1^4(V_1 - V_K) \\ &\quad -g_{L,1}(V_1 - V_L) - g_c(V_1 - V_2) \\ C_2\dot{V}_2 &= I_2 - g_{Na,2}m_2^3h_2(V_2 - V_{Na}) \\ &\quad -g_{K,2}n_2^4(V_2 - V_K) \\ &\quad -g_{L,2}(V_2 - V_L) - g_c(V_2 - V_1). \end{aligned} \tag{6}$$

The gating variables are governed by two sets of three ODEs

$$\begin{aligned} \dot{m}_i &= a_m(V_i)(1 - m_i) - b_m(V_i)m_i \\ \dot{h}_i &= a_h(V_i)(1 - h_i) - b_h(V_i)h_i \\ \dot{n}_i &= a_n(V_i)(1 - n_i) - b_n(V_i)n_i \end{aligned} \tag{7}$$

for $i = 1, 2$. If both neurons are identical (i.e., have the same parameters), we omit the numbering in the parameters (e.g., $C_1 = C_2 =: C$ etc.).

In this paper we consider the case where these coupled neurons are stimulated only by the input current into a single neuron, i.e., the second neuron is stimulated through its interconnection to the first neuron. Without loss of generality we use I_1 as an input current and set $I_2 = 0$.

First, we carry out the simulation using the same parameters and initial values for both neurons as given in Section 2.1. It can be seen in Fig. 3 that there is a synchronization between the two neurons, i.e., $V_1 \approx V_2$. The slightly different behaviour is due to the fact that only neuron 1 is stimulated externally. Nevertheless, the synchronization is achieved via the coupling current (5). From equilibrium considerations of Eq. (6) we see that the synchronization occurs at $I_C = I_1/2$, which is confirmed by the numerical results shown in Fig. 3.

Next, we carry out the simulation using different parameters for the second neuron: $C_2 = 1.2\ \frac{\mu F}{cm^2}$, $g_{Na,2} = 175\ \frac{mS}{cm^2}$, $V_{Na,2} = 115\ mV$, $g_{K,2} = 40\ \frac{mS}{cm^2}$, $V_{Na,2} = -12\ mV$, $g_{L,2} = 0.25\ \frac{mS}{cm^2}$, $V_{L,2} = 12.44\ mV$. The simulation result is shown in Fig. 4. The neurons still synchronize. However, the synchronization results in a strong coupling current I_C between the neurons. For more details on the synchronization of coupled neurons we refer to [21] and references cited there.

System (6)-(7) is a multi-input multi-output system. We focus on two scenarios, where only one current excites the system and only one voltage is measured:

Scenario A I_1 is the input, V_1 is the output,

Scenario B I_1 is the input, V_2 is the output.

The resulting system is a single-input single-output system having an 8-dimensional state-space.

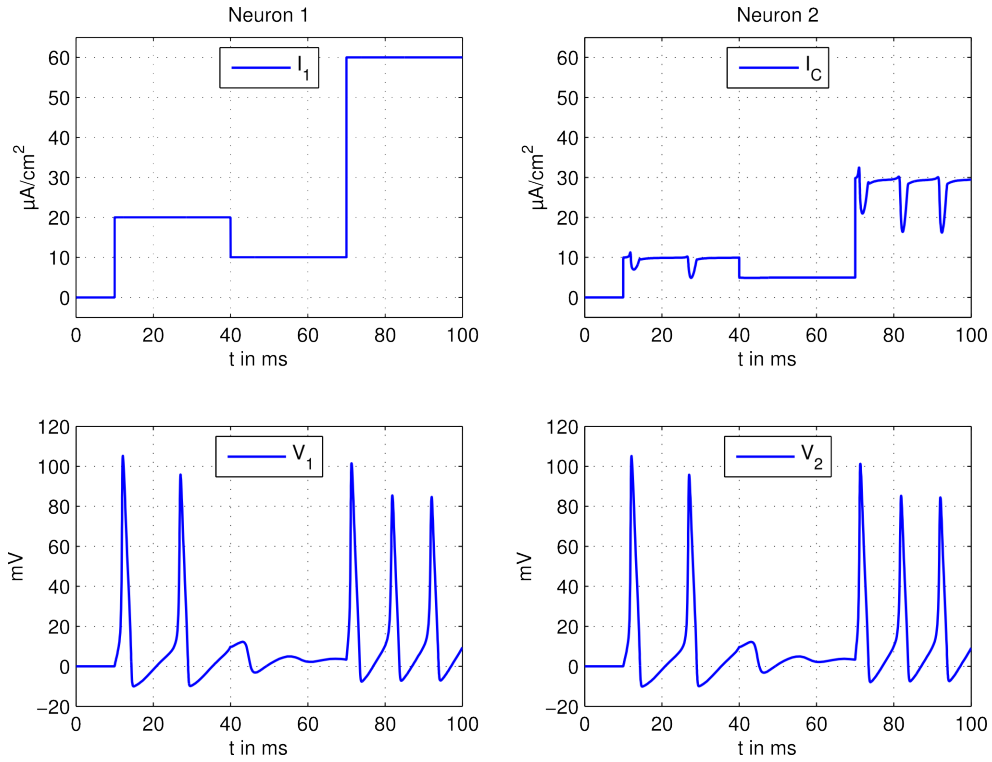

Figure 3: Simulation of coupled neurons with identical parameters

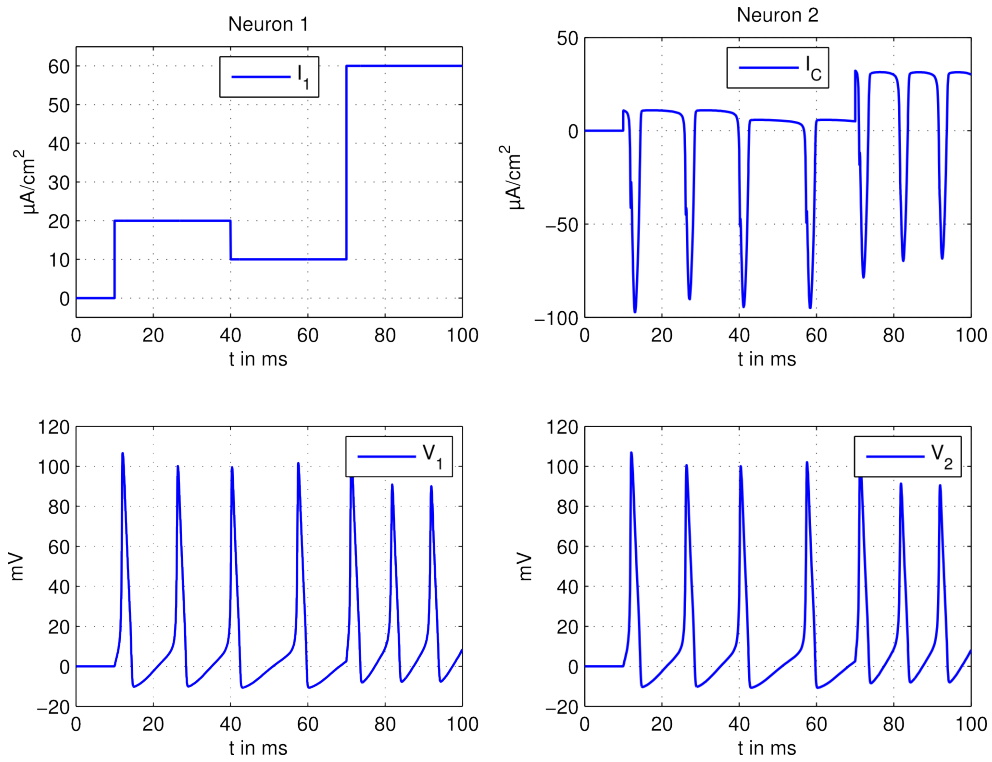

Figure 4: Simulation of coupled neurons with slightly different parameters

3 Control Theoretic Background

3.1 Relative Degree

Both scenarios introduced in Section 2.2 yield a single-input single-output system

$$\dot{x} = f(x) + g(x)u, \quad y = h(x) \tag{8}$$

with two vector fields $f, g : \Omega \to \mathbb{R}^n$ and a scalar field $h : \Omega \to \mathbb{R}$, which are defined on an open subset $\Omega \subseteq \mathbb{R}^n$. All maps are assumed to be sufficiently smooth. The *Lie derivative* of h along f is defined by $L_f h(x) = \mathrm{d}\, h(x) \cdot f(x)$, where $\mathrm{d}\, h(x) = h'(x)$ denotes the gradient of $h(x)$. The Lie derivative of the scalar field h is a scalar field itself. We can recursively define iterated Lie derivatives $L_f^k h(x) = \mathrm{d}\, L_f^{k-1} h(x) \cdot f(x)$ with $L_f^0 h(x) = h(x)$. Mixed Lie derivatives are Lie derivatives along different vector fields, e.g. $L_g L_f h(x) = \mathrm{d}\, L_f h(x) \cdot g(x)$.

We recall the following definition [18, 44]. System (8) is said to have *relative degree* r at $x_0 \in \Omega$ if

1. $L_g L_f^k h(x) = 0$ for $k = 0, \ldots, r-2$ in a neighbourhood of x_0 ,
2. $L_g L_f^{r-1} h(x_0) \neq 0$.

Consider the time derivative of the output y along the dynamics of system (8):

$$\begin{aligned} \dot{y} &= \tfrac{\partial h(x)}{\partial x} \tfrac{\mathrm{d}\, x}{\mathrm{d}\, t} \\ &= \mathrm{d}\, h(x)\,(f(x) + g(x)u) \\ &= L_f h(x) + L_g h(x) u. \end{aligned}$$

If $L_g h(x_0) \neq 0$, the relative degree is $r = 1$. In this case, the first time derivative of the output depends explicitly on the input u. If $L_g h(x) \equiv 0$, we consider the next time derivative

$$\begin{aligned} \ddot{y} &= \tfrac{\partial L_f h(x)}{\partial x} \tfrac{\mathrm{d}\, x}{\mathrm{d}\, t} \\ &= \mathrm{d}\, L_f h(x)\,(f(x) + g(x)u) \\ &= L_f^2 h(x) + L_g L_f h(x) u. \end{aligned}$$

If $L_g L_f h(x_0) \neq 0$, the relative degree is $r = 2$. Then, the second time derivative of y depends explicitly on the input u. More generally, the relative degree is the minimum order of a time derivative of the output that depends directly on the input.

3.2 Normal Form

If system (8) has a relative degree $r < n$, there exists a diffeomorphic change of coordinates $(\xi, \eta) = \Phi(x)$ such that system (8) is decomposed into two subsystems. [1] The first subsystem has the form

$$\begin{aligned} \dot{\xi}_1 &= \xi_2 \\ &\vdots \\ \dot{\xi}_{r-1} &= \xi_r \\ \dot{\xi}_r &= \alpha(\xi, \eta) + \beta(\xi, \eta) u \end{aligned} \tag{9}$$

with $\xi = (\xi_1, \ldots, \xi_r)^T$. Moreover, we have the maps $\alpha(\xi, \eta) = L_f^r h(\Phi^{-1}(\xi, \eta))$ and $\beta(\xi, \eta) = L_g L_f^{r-1} h(\Phi^{-1}(\xi, \eta))$, where Φ^{-1} denotes the inverse map of the diffeomorphism Φ. The new coordinates are chosen by $\xi_i = \phi_i(x) = L_f^{i-1} h(x)$ for $i = 1, \ldots, r$. The remaining coordinates $\eta_i = \phi_{r+i}(x)$ can be chosen such that $L_g \phi_{r+i}(x) \equiv 0$ for $i = 1, \ldots, n-r$. Then, the right hand side $q = (q_1, \ldots, q_{n-r})^T$ of the second system

$$\begin{aligned} \dot{\eta}_1 &= q_1(\xi, \eta) \\ &\vdots \\ \dot{\eta}_{n-r} &= q_{n-r}(\xi, \eta) \end{aligned} \tag{10}$$

does not depend explicitly on the input. More precisely, we have $q_i(\xi, \eta) = L_f \phi_{r+i}(\Phi^{-1}(\xi, \eta))$ for $i = 1, \ldots, n-r$. The form (9)-(10) is called *Byrnes-Isidori normal form* [5, 18].

In case of $r = 1$, we have $\xi_1 = h(x) = y$. The normal form (9)-(10) reads as

$$\begin{aligned} \dot{y} &= \alpha(y, \eta) + \beta(y, \eta) u \\ \dot{\eta}_1 &= q_1(y, \eta) \\ &\vdots \\ \dot{\eta}_{n-1} &= q_{n-1}(y, \eta) \end{aligned} \tag{11}$$

with $\alpha(y, \eta) = L_f h(\Phi^{-1}(y, \eta))$ and $\beta(y, \eta) = L_g h(\Phi^{-1}(y, \eta))$.

In case of $r = 2$, we additionally have $\xi_2 = L_f h(x) = \dot{y}$, i.e., $\xi = (y, \dot{y})^T$. Writing the two-dimensional first subsystem (9) as one second order ODE, the transformed system becomes

$$\begin{aligned} \ddot{y} &= \alpha(y, \dot{y}, \eta) + \beta(y, \dot{y}, \eta) u \\ \dot{\eta}_1 &= q_1(y, \dot{y}, \eta) \\ &\vdots \\ \dot{\eta}_{n-2} &= q_{n-2}(y, \dot{y}, \eta) \end{aligned} \tag{12}$$

with $\alpha(y, \dot{y}, \eta) = L_f^2 h(\Phi^{-1}(y, \dot{y}, \eta))$ and $\beta(y, \dot{y}, \eta) = L_g L_f h(\Phi^{-1}(y, \dot{y}, \eta))$.

[1] Formally, the diffeomorphism $\Phi : \Omega \to \mathbb{R}^n$ is a map between open subsets of $\mathbb{R}^n$. To simplify the notation, we write $(\xi, \eta) = \Phi(x)$, where the point $x \in \Omega$ is mapped into the pair $(\xi, \eta) \in \mathbb{R}^r \times \mathbb{R}^{n-r}$, which is isomorphic to the vector space $\mathbb{R}^n$.

3.3 Unknown Input Observer

The usage of the Byrnes-Isidori normal form (9)-(10) to design an unknown input observer has been suggested in [26, 27, 40]. The design procedure is applicable if system (8) has the relative degree $r = 1$, i.e., if it is transformable into (11). The observer consists of a copy of the $(n-1)$-dimensional second subsystem of (11). The original state is recovered using the output and the inverse change of coordinates. More precisely, the observer reads as

$$\begin{aligned} \dot{\hat{\eta}} &= q(y, \hat{\eta}), \quad \hat{\eta}(0) = \hat{\eta}_0 \in \mathbb{R}^{n-1} \\ \hat{x} &= \Phi^{-1}(y, \hat{\eta}). \end{aligned} \tag{13}$$

For the observer (13) to converge we have to ensure that $\hat{\eta}(t) \to \eta(t)$ for $t \to \infty$ independent of the initial value $\hat{\eta}(0) = \hat{\eta}_0$. The observation error $\tilde{\eta} = \eta - \hat{\eta}$ of (11) and (13) is governed by the error dynamics

$$\dot{\tilde{\eta}} = q(y, \eta) - q(y, \hat{\eta}), \quad \tilde{\eta}(0) = \eta(0) - \hat{\eta}(0). \tag{14}$$

We have to investigate the stability of the equilibrium point $\tilde{\eta} = 0$. Since we have no observer gain, the second subsystem must exhibit an intrisic stability property. Let S be a continuously differentiable, positive definite and radially unbounded function defined on the state space of (14). We assume that

$$\frac{\partial S}{\partial \tilde{\eta}}(q(y, \eta) - q(y, \hat{\eta})) < 0 \quad \text{for all} \quad \tilde{\eta} \neq 0 \tag{15}$$

and all admissibe y. This means that S is a global Lyapunov function of (14), i.e., the equilibrium $\tilde{\eta} = 0$ is globally asymptotically stable. As a matter of fact, Ineq. (15) can be interpreted as a nonlinear detectability condition [2].

In case of relative degree $r = 2$, it is tempting to proceed similar as above. One might use a copy of the $(n-2)$-dimensional subsystem of (12):

$$\begin{aligned} \dot{\hat{\eta}} &= q(y, \dot{y}, \hat{\eta}), \quad \hat{\eta}(0) = \hat{\eta}_0 \in \mathbb{R}^{n-2} \\ \hat{x} &= \Phi^{-1}(y, \dot{y}, \hat{\eta}). \end{aligned} \tag{16}$$

Eq. (14) and Ineq. (15) can easily be modified accordingly. However, we encounter two difficulties. First, we measure y but not $\dot{y}$. A numerically reliable reconstruction $\dot{\hat{y}}$ of $\dot{y}$ from discrete points of y is not easy. Second, the observer (16) might not converge. In particular, high frequency output signals increase the difficulties to reconstruct $\dot{y}$. As for asymptotic considerations, we get $\dot{\hat{y}}(t) \not\to \dot{y}(t)$ for $t \to \infty$, by which the observer (16) cannot converge. In fact, it has been pointed out in [26, 40] that the relative degree $r = 1$ is a *necessary* condition for the convergence of an unknown input observer. In case of $r > 1$ we have to accept a *non-asymptotic* estimation [33].

3.4 Observer Based Input Reconstruction

The unknown input observers (13) and (16) reconstruct the state vector x without measurement of the input u. The unknown input observers use only the dynamics (10) of the second subsystem of the Byrnes-Isidori normal form. Now, we want to estimate the input u. To achieve this, we also take of the first subsystem (9) into account.

In case of $r = 1$, we solve the first equation of (11) w.r.t. u. Since the relative degree is assumed to be well-defined we have $\beta \neq 0$. This results in

$$u = \frac{\dot{y} - \alpha(y, \eta)}{\beta(y, \eta)}. \tag{17}$$

The internal state vector η is not directly measured, but reconstructed with the unknown input observer (13). Under the assumption that the observer (13) converges we can replace the exact state η of the second subsystem (10) by its estimate $\hat{\eta}$ and obtain an estimate $\hat{u}$ of the exact input u by

$$\hat{u} = \frac{\dot{y} - \alpha(y, \hat{\eta})}{\beta(y, \hat{\eta})}. \tag{18}$$

Obviously, the convergence $\hat{\eta} \to \eta$ for $t \to \infty$ of the observer (13) implies $\hat{u} \to u$, provided y and $\dot{y}$ are known.

We can proceed similarly for $r = 2$. Using the first equation of (12) and replacing η by $\hat{\eta}$ from the observer (16) yields

$$\hat{u} = \frac{\ddot{y} - \alpha(y, \dot{y}, \hat{\eta})}{\beta(y, \dot{y}, \hat{\eta})}. \tag{19}$$

The estimated input $\hat{u}$ in (18) and (19) depends explicitly on the measured output y and its time derivatives. Therefore, the estimation $\hat{u}$ of u is directly affected by measurement noise. To suppress this noise we suggest the use of a low order low-pass filter having the continuous time transfer function

$$T(s) = \frac{a_0}{a_0 + a_1 s + \cdots + a_{m-1} s^{m-1} + s^m}. \tag{20}$$

The coefficients $a_0, \ldots, a_{m-1} > 0$ have to be chosen such that all poles of (20) have negative real parts. There are several standard methods available from filter design such as Bessel or Butterworth filter [47].

In the time domain, the low-pass filter (20) is applied to the estimates (18) or (19) via

$$\bar{u}(t) = T(\tfrac{\mathrm{d}}{\mathrm{d}t}) \circ \hat{u}(t) \tag{21}$$

resulting in the filtered estimate $\bar{u}$ of the input current u. From the viewpoint of implementation, we would realize (20) with (21) as a discrete time state-space system. By an appropriate implementation of the filter (20), the explicit differentiation of y in (18) can be circumvented [39].

3.5 Derivative Estimation

Only the scalar-valued output y of our system (8) is available for measurement. More precisely, the output is measured at discrete sample points t_i, i.e., we have the values $y(t_0), y(t_1), \ldots$ as a series, but not $y : [0, \infty) \to \mathbb{R}$ as a function. For a practical implementation, we assume equidistant sampling with the period $\Delta t = t_{i+1} - t_i$ for all integers $i \geq 0$.

As shown in Eqs. (18) and (19), the reconstruction of the input u requires the knowledge of first and second order time derivatives $\dot{y}$ and $\ddot{y}$, respectively, of the measured output y. A simple way to obtain derivative values from sampled data are finite difference schemes such as the backward difference

$$\dot{y}(t_i) \approx \frac{y(t_i) - y(t_{i-1})}{\Delta t}.$$

This so-called numeric differentiation is not reliable due to cancellation and truncation errors [14, Chapter 1]. In the following, we introduce two alternatives in order to avoid these problems.

3.5.1 State-Variable Filter

The idea behind the state-variable filter can be explained as follows [17, 53]: We apply a low-pass filter with a transfer function of the form (20) to the signal y, that is

$$\bar{y}(t) = T(\tfrac{\mathrm{d}}{\mathrm{d}t}) \circ y(t). \tag{22}$$

The filter is implemented as a state-space system in such a manner, that the states are derivatives of the filter output. Although the filter distorts the measured signal, we obtain at least exact derivative values of this filtered signal $\bar{y}$.

To go into the details, the filter transfer function (20) is implemented as a state-space system in observability canonical form

$$\begin{aligned} \dot{z} &= \begin{pmatrix} 0 & 1 & 0 & \cdots \\ \vdots & 0 & \ddots & \ddots \\ \vdots & \vdots & \ddots & 1 \\ -a_0 & -a_1 & \cdots & -a_{m-1} \end{pmatrix} z + \begin{pmatrix} 0 \\ \vdots \\ 0 \\ a_0 \end{pmatrix} y \\ \bar{y} &= \begin{pmatrix} 1 & 0 & \cdots & 0 \end{pmatrix} z \end{aligned} \tag{23}$$

with the state vector $z = (z_1, \ldots, z_m)^T$. Starting with the output $\bar{y} = z_1$, total time derivatives along the dynamics of (22) result in

$$\begin{aligned} \bar{y} &= z_1 \\ \dot{\bar{y}} &= z_2 \\ \ddot{\bar{y}} &= z_3 \\ &\vdots \\ \bar{y}^{(m-1)} &= z_m \\ \bar{y}^{(m)} &= -a_0 z_1 - \cdots - a_{m-1} z_m + a_0 y. \end{aligned} \tag{24}$$

The state-variable filter (23) should be implemented as a discrete time state-space system using zeroth order hold time discretization [10].

3.5.2 Algebraic Derivative Estimation

The concept of algebraic derivative estimation was introduced in [13]. A real-time implementation was reported in [54]. The following derivation is similar to [24].

The measured output $y(t)$ is given at discrete sample points $t \in \{t_0, t_1, \ldots\}$. The signal y is modeled by a smooth signal $\hat{y}$, which is locally around t_i represented as a truncated Taylor series

$$\hat{y}(t) = \sum_{k=0}^{m} \frac{y_k}{k!} (t - t_i)^k \tag{25}$$

of order m with the Taylor coefficients $y_0, \ldots, y_m$. Clearly, time derivatives of the signal (25) at t_i are related to the Taylor coefficients in the following way:

$$y_k = \frac{\mathrm{d}^k}{\mathrm{d}\,t^k} \hat{y}(t)|_{t_i}. \tag{26}$$

We want to find the Taylor coefficients of (25) such that the cost functional

$$J = \frac{1}{2} \int_{t_i - \Delta T}^{t_i} [y(t) - \hat{y}(t)]^2 \,\mathrm{d}\,t \tag{27}$$

is minimized over a time frame ΔT. For practical reasons we assume that width of the time frame ΔT is an integral multiple of the sampling period Δt, i.e., $\Delta T = N \cdot \Delta t$ and $t_i - \Delta T = t_{i-N}$. The minimim of the cost functional J is obtained from

$$\begin{aligned} \frac{\partial J}{\partial y_j} &= \frac{\partial}{\partial y_j} \tfrac{1}{2} \int_{t_{i-N}}^{t_i} \left[y(t) - \sum_{k=0}^{m} \tfrac{y_k}{k!} (t - t_i)^k \right]^2 \mathrm{d}\,t \\ &= \tfrac{1}{2} \int_{t_{i-N}}^{t_i} \frac{\partial}{\partial y_j} \left[y(t) - \sum_{k=0}^{m} \tfrac{y_k}{k!} (t - t_i)^k \right]^2 \mathrm{d}\,t \\ &= -\int_{t_{i-N}}^{t_i} \left[y(t) - \sum_{k=0}^{m} \tfrac{y_k}{k!} (t - t_i)^k \right] \tfrac{(t-t_i)^j}{j!} \,\mathrm{d}\,t \\ &\overset{!}{=} 0 \end{aligned}$$

for $j = 0, \ldots, m$, which yields a system of $m+1$ equations in the $m+1$ variables $y_0, \ldots, y_m$. The substitution $\tau = t - t_i$ together with an symbolic integration of the Taylor series yields

$$\frac{1}{j!} \int_{\Delta T}^{0} y(\tau + t_i) \tau^j \, \mathrm{d}\, \tau = \sum_{k=0}^{m} (-1)^{j+k} \frac{\Delta T^{k+j+1}}{k+j+1} y_k$$

for $j = 0, \ldots, m$. Finally, the Taylor coefficients $y_0, \ldots, y_m$ can be obtained as the solution of the system of linear equations

$$\Phi \cdot \begin{pmatrix} y_0 \\ \vdots \\ y_m \end{pmatrix} = \begin{pmatrix} \int_{-\Delta T}^{0} y(\tau + t_i) \, \mathrm{d}\, \tau \\ \vdots \\ \frac{1}{m!} \int_{-\Delta T}^{0} y(\tau + t_i) \tau^m \, \mathrm{d}\, \tau \end{pmatrix}, \tag{28}$$

where the entries Φ_{ij} of the matrix $\Phi \in \mathbb{R}^{(m+1)\times(m+1)}$ have the form

$$\Phi_{ij} = (-1)^{i+j} \frac{\Delta T^{i+j+1}}{i+j+1}. \tag{29}$$

The matrix Φ is constant and can be inverted off-line. The integrals on the right-hand side of (28) are computed numerically using the sample points (e.g. using the trapezoidal rule). As a matter of fact, these integration can easily be implemented recursively. Solving (28) w.r.t. the Taylor coefficients $y_0, \ldots, y_m$, we obtain the desired derivatives estimates of the output y at t_i from (26).

4 Current Estimation for Coupled Neurons

The preceding control theoretic background serves as basis for the development of the unknown input observers for each Scenario A and B. Divided by the scenarios, in the following two subsection each state-space system will be analyzed regarding relative degree and normal form. Furthermore, the unknown input observers will be derived from the normal forms and finally, their convergence will be investigated.

For both scenarios the state-space vector is defined as follows:

$$\begin{aligned} x &= (x_1, x_2, x_3, x_4, x_5, x_6, x_7, x_8)^T \\ &= (V_1, h_1, m_1, n_1, V_2, h_2, m_2, n_2)^T. \end{aligned} \tag{30}$$

The vector fields $f, g : \mathbb{R}^8 \to \mathbb{R}^8$ of system (8) given by Eqs. (6)-(7) have the form

$$\begin{aligned} f(x) &= (f_1(x), \cdots, f_8(x))^T, \\ g(x) &= \left(\tfrac{1}{C_1}, 0, \cdots, 0\right)^T. \end{aligned}$$

Note that the vector field g is constant.

4.1 Scenario A

This section focuses on the case of two coupled neurons described as in (8) with $I_1 = u$ being the input and $V_1 = y = h_A(x)$ being the output. The system has a relative degree of one, which results as follows:

$$\begin{aligned} L_g h_A(x) &= h_A'(x) g(x) \\ &= (1, 0, \cdots, 0)\, g(x) \\ &= \tfrac{1}{C_1} \neq 0. \end{aligned} \tag{31}$$

Hence, the normal form of the system in Scenario A corresponds to (11), i.e., the given system (6)-(7) is already in normal form for the input $u = I_1$ and the output $y = V_1$. For the sake of simplicity, the original notation (6)-(7) of the coupled system will be used in the following calculations.

The goal of the observer design is getting a convergent estimation

$$\lim_{t \to \infty} \tilde{I}_1 = 0,$$

where $\tilde{I}_1 := I_1 - \hat{I}_1$ denotes the estimation error of the input current I_1. This analysis is carried out in different steps.

Using Lyapunov methods, it has been shown in [38] that the estimated gating variables $\hat{h}$, $\hat{m}$, $\hat{n}$ of the corresponding neuron converge if the membrane voltage V_1 is measured correctly. In other words, the observer state variables of the internal dynamics of neuron one converge, i.e., $\hat{h}_1 \to h_1$, $\hat{m}_1 \to m_1$ and $\hat{n}_1 \to n_1$ for $t \to \infty$. It follows from the first equation of (6) that

$$\lim_{t \to \infty} \left(I_1 - \hat{I}_1 \right) = -g_C \left(V_2 - \hat{V}_2 \right).$$

This implies that the convergence of $\hat{V}_2$ to V_2 is required for a precise measurement of I_1.

Since V_2 is not exactly known through measurement, the convergence of the gating variables $\hat{h}_2$, $\hat{m}_2$ and $\hat{n}_2$ cannot be proved in the same manner as demonstrated in [38] for the gating variables of the

first neuron. However, we will show that the absolute error $|V_2 - \hat{V}_2|$ and therefore $|\tilde{I}_1|$ is bounded for $t \to \infty$.

The ODE for the observer state $\hat{V}_2$ corresponds to the second equation in (6) with $\hat{V}_2$, $\hat{h}_2$, $\hat{m}_2$ and $\hat{n}_2$ instead the actual states. Rearrangement of the resulting equation leads to

$$\dot{\hat{V}}_2 = -\bar{g}(t)\hat{V}_2 + \hat{u}_a(t) - u_b(t) \tag{32}$$

with

$$\bar{g}(t) = \frac{1}{C_2}\left[g_{Na,2}\hat{m}_2^3\hat{h}_2 + g_{K,2}\hat{n}_2^4 + g_{L,2} + g_C\right]$$

and

$$\begin{aligned}\hat{u}_a(t) = &\frac{1}{C_2}\left[g_{Na,2}\hat{m}_2^3\hat{n}_2 V_{Na,2}\right.\\ &\left.+g_{K,2}\hat{h}_2^4 V_{2,K} + g_{L,2}V_{L,2}\right],\\ u_b(t) = &\frac{g_C}{C_2}V_1.\end{aligned}$$

As stated in [15], the values for gating variables remain in the range [0,1]. Direct calculation shows that $\bar{g}(t)$ is bounded by

$$0 < \bar{g}_{min} \le \bar{g}(t) \le \bar{g}_{max} \tag{33}$$

with

$$\begin{aligned}\bar{g}_{min} &= \tfrac{1}{C_2}\left(g_{L,2} + g_C\right),\\ \bar{g}_{max} &= \tfrac{1}{C_2}\left(g_{Na,2} + g_{K,2} + g_{L,2} + g_C\right).\end{aligned}$$

In case of a constant function $\bar{g}(t) = \bar{g}_0$, Eq. (32) represents an linear inhomogeneous differential equation with the solution

$$\hat{V}_2(t) = \hat{V}_2(0)e^{-\bar{g}_0 t} + \int_0^t e^{\bar{g}_0(\tau - t)}\left[\hat{u}_a(\tau) - u_b(\tau)\right]\mathrm{d}\tau.$$

For $t \to \infty$, the influence of the initial value disappears since $\bar{g}_0 \in [\bar{g}_{min}, \bar{g}_{max}]$ implies $\bar{g}_0 > 0$. Consequently, the asymptotics are described by

$$\lim_{t\to\infty}\hat{V}_2(t) = \int_0^\infty e^{\bar{g}_0(\tau - t)}\left[\hat{u}_a(\tau) - u_b(\tau)\right]\mathrm{d}\tau.$$

Equally, the general solution for V_2 can be found. Hence, the estimation error is governed by

$$\lim_{t\to\infty}\left(V_2(t) - \hat{V}_2(t)\right) = \int_0^\infty e^{\bar{g}_0(\tau - t)}\left[u_a(\tau) - \hat{u}_a(\tau)\right]\mathrm{d}\tau \tag{34}$$

with

$$\begin{aligned}u_a(t) = \frac{1}{C_2}&\left[g_{Na,2}m_2^3 h_2 V_{Na,2}\right.\\ &\left.+g_{2,K}n_2^4 V_{K,2} + g_{L,2}V_{L,2}\right].\end{aligned}$$

Furthermore, with the knowledge h_i, m_i, $n_i \in [0,1]$ $(i = 1, 2)$, an upper bound of (34) can be found as follows:

$$\begin{aligned}&\lim_{t\to\infty}\left|V_2(t) - \hat{V}_2(t)\right| =\\ &= \lim_{t\to\infty}\left|\int_0^t e^{\bar{g}_0(\tau-t)}\left[u_a(\tau) - \hat{u}_a(\tau)\right]\mathrm{d}\tau\right|\\ &\le \lim_{t\to\infty}\left|\int_0^t \frac{1}{C_2}\left[g_{Na,2}V_{Na,2} + g_{K,2}V_{K,2}\right]e^{\bar{g}_0(\tau-t)}\mathrm{d}\tau\right|\\ &\le \lim_{t\to\infty}\frac{\left|g_{2,Na}V_{2,Na} + g_{2,K}V_{2,K}\right|}{C_2\bar{g}_0}\left|1 - e^{-\bar{g}_0 t}\right|\\ &\le \frac{\left|g_{2,Na}V_{2,Na} + g_{2,K}V_{2,K}\right|}{g_{2,L} + g_C} =: \tilde{V}_{\infty,max}.\end{aligned}$$

With the neuron parameters from Section 2.1, the upper bound results in

$$\tilde{V}_{\infty,max} = \frac{\left|120\cdot 115 + 36\cdot(-12)\right|}{0.3 + 100}mV \approx 133.3mV.$$

In practice, $\tilde{V}_2$ stays clearly below this theoretical upper bound as demonstrated in Fig. 5. This implies good approximation $\hat{I}_1 \approx I_1$.

As final step, the observer is augmented by a filter for the estimated signal $\hat{u} = \hat{I}_1$. The necessity of filtering has already been addressed in Section 3.4. Using Eq. (21), the filtered input current estimate $\bar{I}_1$ results from

$$\begin{aligned}\bar{I}(t) &= T\left(\tfrac{\mathrm{d}}{\mathrm{d}t}\right)\circ\hat{I}_1(t)\\ &= T\left(\tfrac{\mathrm{d}}{\mathrm{d}t}\right)\circ\Big(C_1\dot{V}_1(t)\\ &\quad + F(V_1, \hat{V}_2, h_1, m_1, n_1)\Big)\end{aligned} \tag{35}$$

with

$$\begin{aligned}F(V_1, \hat{V}_2, h_1, m_1, n_1) = &\, g_{Na,1}\hat{m}_1^3\hat{h}_1(V_1 - V_{Na,1})\\ &+ g_{K,1}\hat{n}_1^4(V_1 - V_{K,1})\\ &+ g_{L,1}(V_1 - V_{L,1}) - g_C(V_1 - \hat{V}_2).\end{aligned}$$

As stated in Section 3.4, the time derivative $\dot{V}_1$ of V_1 can be obtained directly from the filter. More precisely, we apply the filter transfer function (20) to F, and the modified transfer function

$$T_{\text{diff}}(s) = \frac{a_0 s}{a_0 + a_1 s + \cdots + a_{m-1}s^{m-1} + s^m},$$

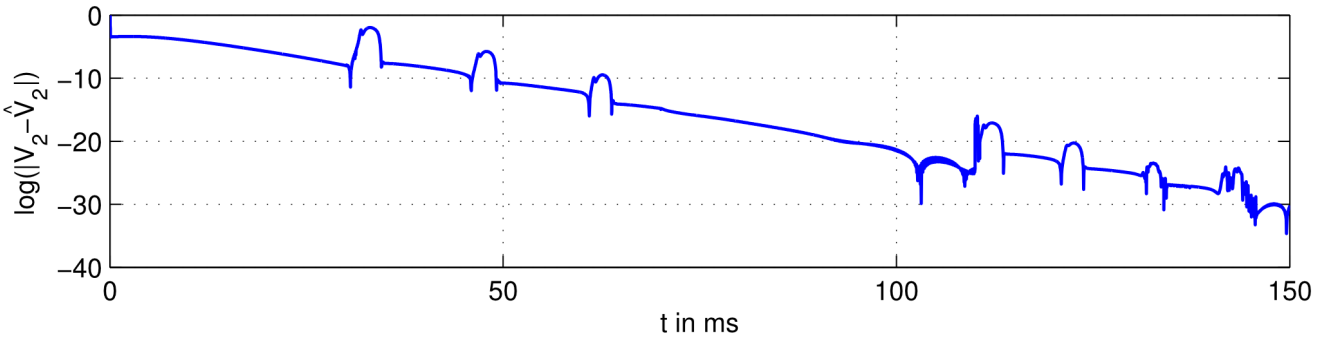

Figure 5: Estimation error of V_2 using identical neurons with different initial values in the observer ($\hat{V}_2(0) = 50\,mV \neq V_2(0) = 0\,mV$ and $\hat{h}_2(0) = 0 \neq h_2(0)$ etc.)

which carries out a differentiation, to $C_1 V_1(t)$. This results in

$$\begin{aligned} \bar{I}(t) &= T\left(\tfrac{\mathrm{d}}{\mathrm{d}t}\right) \circ \left(C_1 \dot{V}_1(t) + F(\cdots)\right) \\ &= T\left(\tfrac{\mathrm{d}}{\mathrm{d}t}\right) \circ (F(\cdots)) + C_1 T_{\text{diff}}\left(\tfrac{\mathrm{d}}{\mathrm{d}t}\right) \circ V_1(t). \end{aligned}$$

Figure 6 depicts the application of this filter scheme using a fourth order Bessel filter with the cut-off frequency $\omega_g = 0.3\ kHz$. Even with the influence of measurement noise, the observer yields a reasonable estimation for the input current of neuron one.

To sum up, we derived a theoretical upper bound for the estimation error. In practice the designed observer shows good and stable estimations.

4.2 Scenario B

Again, the goal is getting a convergent estimation for the input current of neuron one, i.e., $\hat{I}_1 \to I_1$. Similar to Scenario A, this section starts with the computation of the relative degree and the elaboration of the Byrnes-Isidori normal form. With this preliminary work, we will carry out the observer design and analyse its convergence.

Here, the input-output configuration $u = I_1$ and $y = V_2 = h_B(x)$ results in the following first Lie-derivative of the output map h_B along the input vector field g:

$$\begin{aligned} L_g h_B(x) &= h_B'(x) g(x) \\ &= (0,0,0,0,1,0,0,0)\, g(x) = 0 \end{aligned}$$

As explained in Section 3.1, the first mixed Lie-derivative has to be taken into account:

$$\begin{aligned} L_g L_f h_B(x) &= L_g\left((h'(x) f(x))\right) \\ &= L_g f_5(x) \\ &= \tfrac{g_C}{C_1 C_2} \neq 0. \end{aligned}$$

Consequently, in Scenario B the relative degree of the system is two. Further, its normal form corresponds to (12) with the diffeomorphisms

$$\Phi(x) = (x_5, f_5(x), x_2, x_3, x_4, x_6, x_7, x_8),^T \tag{36}$$

whose inverse is given by

$$\Phi^{-1} = (\Phi_1^{-1}, \eta_1, \eta_2, \eta_3, y, \eta_4, \eta_5, \eta_6)^T \tag{37}$$

with the first component

$$\begin{aligned} \Phi_1^{-1} &= \Phi_1^{-1}(y, \dot{y}, \eta) \\ &= y + \tfrac{1}{g_C}\left[C_2 \dot{y} + g_{Na,2}\eta_4 \eta_5^3 (y - V_{Na,2})\right. \\ &\quad \left. + g_{K,2}\eta_6^4 (y - V_{K,2}) + g_{L,2}(y - V_{L,2})\right]. \end{aligned} \tag{38}$$

As mentioned before, a relative degree of one is a necessary condition for an asymptotic estimation with an unknown input observer under the assuption that only y is measured. Nevertheless, if one assumes an exact estimation of the time derivatives $\dot{\hat{y}}$ and $\ddot{\hat{y}}$ of the measured output signal $y = V_2$, the proof of convergence in $\hat{I}_1$ succeeds. This results from a special form of the internal dynamics as described below.

The comparison of (6) and (12) with (30) and (36) taken into account shows that η_4, η_5 and η_6 correspond to h_2, m_2 and n_2, respectively. Furthermore, their state equations are only functions in $y = V_2$. For the observer states $\hat{\eta}_i$ ($i = 4, 5, 6$) follows that these states converge, since $\hat{y} = y$ is exactly known [38].

To continue, a close look at Eq. (38) reveals that the estimated state $\hat{x}_1 = V_1 = \Phi_1^{-1}$ is just a function in y, $\dot{y}$ and $\hat{\eta}_4, \ldots, \hat{\eta}_6$. Since the estimates of these states are known to converge, it follows that $\hat{x}_1 \to x_1$ holds.

Finally, only the convergence of $\hat{\eta}_1, \ldots, \hat{\eta}_3$ is undetermined. These states correspond to $\hat{h}_1$, $\hat{m}_1$ and

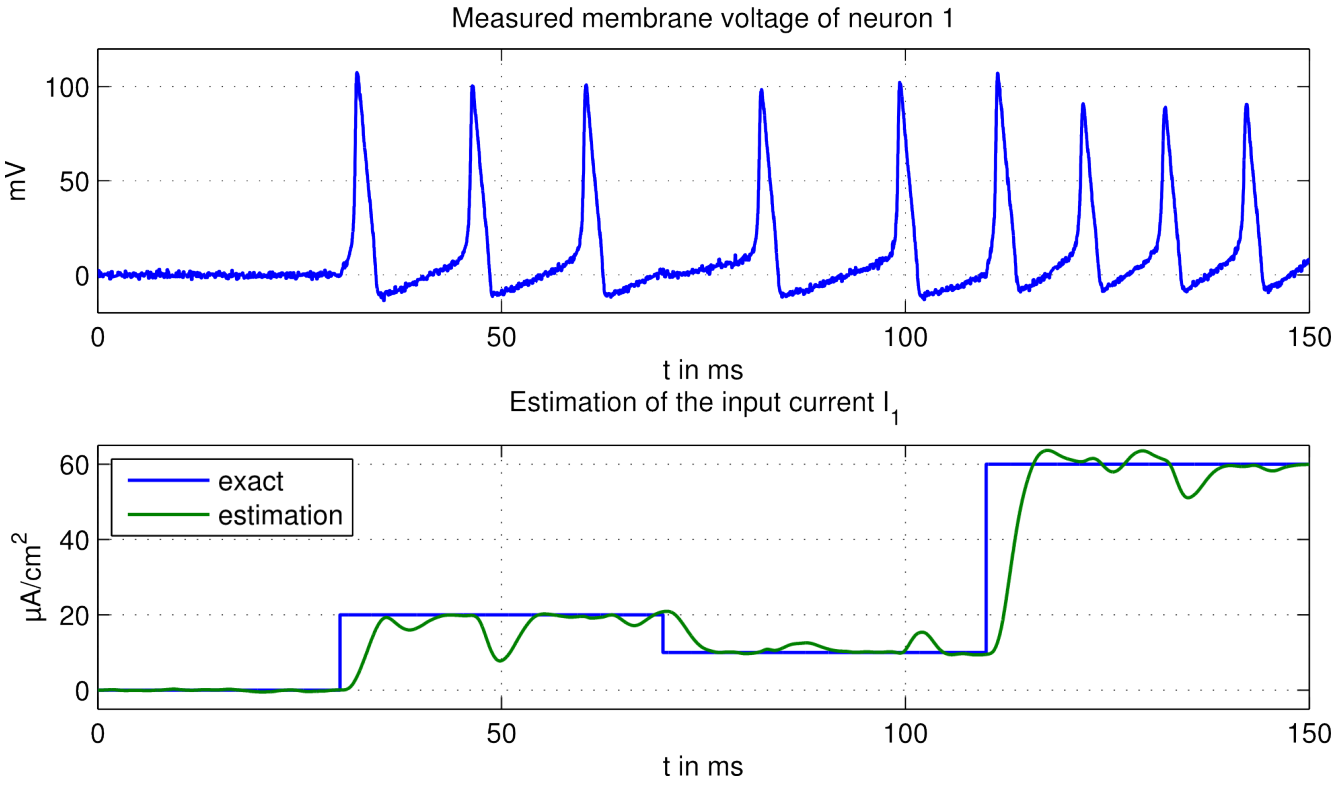

Figure 6: Simulation of the observer for Scenario A with non-identical neurons and measurement noise

$\hat{m}_1$, respectively. Equivalent to neuron two and as stated in [38], for neuron one $\hat{\eta}_i \to \eta_i$ $(i = 1, 2, 3)$ holds due to $\hat{V}_1 \to V_1$.

To sum up, all observer states y, $\dot{y}$ and $\hat{\eta}$ are either exactly known from measurement or converge, respectively. Therefore, a convergent estimation of the input current of neuron one can be obtained by (19). Similar to Scenario A, filtering the estimated signal $\hat{u}$ as in (21) is suitable to suppress the negative impacts of measurement noise.

To conclude Scenario B, Figure 7 shows the results of the designed observer with both algebraic derivative estimation and state-variable filtering. The filter for smoothing $\hat{I}_1$ uses $\omega_g = 0.3\ kHz$, the state variable filter for the derivative estimation $\omega_g = 100\ kHz$. The parameters for the algebraic deviation estimation are $\Delta T = 0.05\ ms$ and the polynomial order is 2. Each method yields reasonable estimations of I_1. However, algebraic estimation suffers slightly from its moving window (ΔT), which comes into effect at spikes of the action potentials. All in all, the observer design has been proven to yield good results.

5 Conclusion

In this paper we suggested a control-theoretic approach for the model based estimation of the current input of neurons. More precisely, we considered a pair of electrically coupled neurons, where an input current is estimated measuring one membrane voltage. In particular, we presented a combination of nonlinear state observers and linear filters. We analyzed the convergence as well as asymptotic properties of our estimation schemes. Moreover, we also discussed the performance limitations due to the system's structure and the accuracy of required derivative estimations.

Acknowledgements: The first author would like to thank Assistant Professor Pranay Goel (Indian Institute of Science Education and Research, Pune), who brought the problem of current estimation for neurons to his attention.

References:

[1] L. Abbott and E. Marder, Modeling Small Networks, in C. Koch and I. Segev (eds.): *Methods*

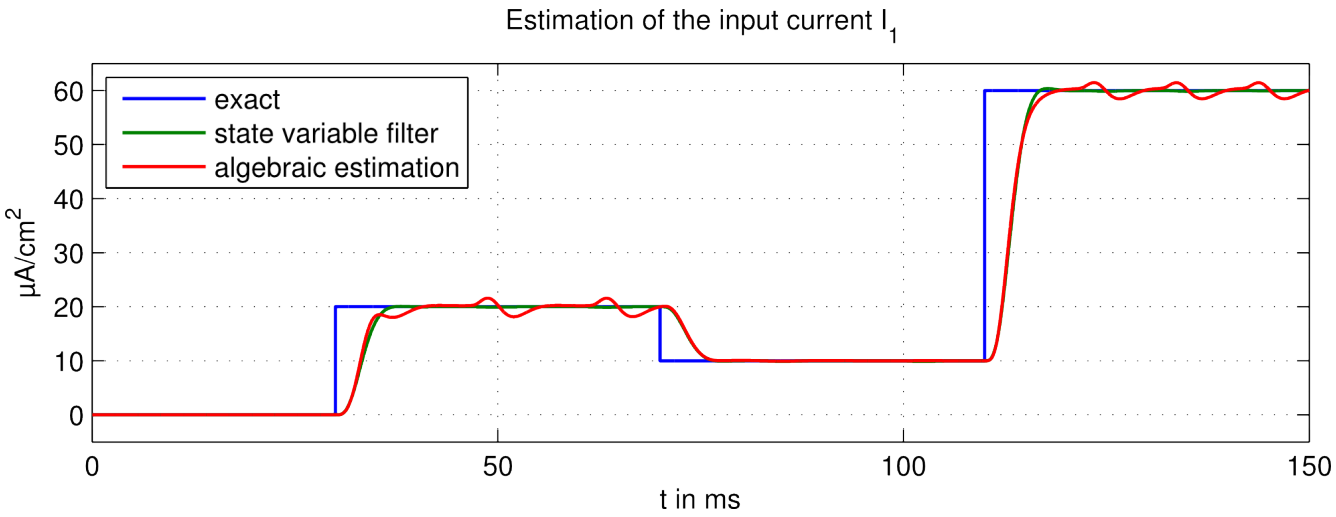

Figure 7: Simulation of the observer for Scenario B with non-identical neurons

in Neuronal Modeling, MIT Press, Cambridge, 1998, pp. 361–410.

[2] G. L. Amicucci and S. Monaco, On nonlinear detectability, *Journal of the Franklin Institue* 335B(6), 1998, pp. 1105–1123.

[3] O. Bernard, A. Sciandra and G. Sallet, A non-linear software sensor to monitor the internal nitrogen quota of phytoplanktonic cells, *Oceanologica Acta* 24(5), 2001, 435–442.

[4] S. P. Bhattacharyya, Observer design for linear systems with unknown inputs, *IEEE Trans. on Automatic Control* AC-23(3), 1978, pp. 483–484.

[5] C. I. Byrnes and A. Isidori, Asymptotic stabilization of minimum phase nonlinear systems, *IEEE Trans. on Automatic Control* 36(10), 1991, pp. 1122–1137.

[6] T. R. Chay and J. Keizer, Minimal model for membrane oscillations in the pancreatic β-cell, *Biophysiological Journal* 42, 1983, pp. 181–190.

[7] K. S. Cole, *Membranes, Oins and Impulses: A Chapter of Classical Biophysics*, University of California Press, Berkeley, CA, USA, 1968.

[8] J. A. Connor and C. F. Stevens, Prediction of repetitive firing behaviour from voltage clamp data on an isolated neurone soma, *Journal of Physiology* 213, 1971, pp. 31–53.

[9] M. Darouach, Z. Zasadzinski and S. J. Xu, Full-order observers for linear systems with unknown inputs, *IEEE Trans. on Automatic Control* 39(3), 1994, pp. 606–609.

[10] R. A. DeCarlo, *Linear systems: a state variable approach with numerical implementation*, Prentice-Hall, Inc., Upper Saddle River, NJ, USA, 1989.

[11] A. S. Finkel and P. W. Gage, Conventional voltage-clamping with two intracellular microelectrodes, in T. G. Smith, H. Lecar, S. J. Redman and P. W. Gage (eds.), *Voltage and patch Clamping with Microelectrodes*, William & Wilkins, Baltimore, USA, 1985, pp. 47–94.

[12] R. FitzHugh, Impulses and physiological states in theoretical models of nerve membrane, *Biophysical Journal* 1, 1961, pp. 445–466.

[13] M. Fliess and H. Sira-Ramírez, An algebraic framework for linear identification, *ESIAM Contr. Opt. Calc. Variat.* 9, 2003.

[14] A. Griewank and A. Walther, *Evaluating Derivatives: Principles and Techniques of Algorithmic Differentiation*, SIAM, 2nd edition, 2008.

[15] A. L. Hodgkin and A. F. Huxley, A quantitative description of membrane current and its application to conduction and excitation in nerve, *Journal of Physiology* 117, 1952, pp. 500–544.

[16] S. Hui and S. H. Żak, Observer design for systems with unknown inputs, *Applied Mathematics and Computer Science* 15(4), 2005, pp. 431–446.

[17] R. Isermann, *Identifikation dynamischer Systeme 2*, Springer, 2nd edition, 1992.

[18] A. Isidori, *Nonlinear Control Systems: An Introduction*, Springer-Verlag, London, 3rd edition, 1995.

[19] R. E. Kalman, A new approach to linear filtering and prediction problems, *Transactions of the ASME Journal of Basic Engineering, Series D* 82, 1960, pp. 35–45.

[20] C. Koch, Ö. Bernander and R. J. Douglas, Do neurons have a voltage or a current threshold for action potential initiation?, *Journal of Computational Neuroscience* 2, 1995, pp. 63–82.

[21] I. S. Labouriau and H. M. Rodrigues, Synchronization of Coupled Equations of Hodgkin-Huxley Type, *Dynamics of Continuous, Discrete and Impulsive Systems* 10(3a), 2003, pp. 463–476.

[22] L. Ljung, Asymptotic behavior of the extended Kalman filter as a parameter estimator for linear systems, *IEEE Trans. on Automatic Control* 24(1), 1979, 36–50.

[23] D. G. Luenberger, Observing the state of a linear system, *IEEE Trans. Mil. Electronics* ME-8(2), 1964, pp. 74–80.

[24] P. Mai and C. Hillermeier, Least-Squares-basierte Ableitungsschätzung: Theorie und Einstellregeln für den praktischen Einsatz, *Automatisierungstechnik* 56(10), 2008, pp. 530–538.

[25] E. A. Misawa and J. K. Hedrick, Nonlinear observers — a state-of-the art survey, *Journal of Dynamic Systems, Measurement, and Control* 111, 1989, pp. 344–352.

[26] J. Moreno, Unknown input observers for SISO nonlinear systems, in *IEEE Conference on Decision and Control*, 2000, volume 1, pp. 790–801.

[27] J. Moreno and E. Rocha-Cózatl, Pasivizaión y existencia de observadores con entradas desconocidas para sistemas no lineales SISO, in *Proc. Conferencia de Ingenieía Eléctrica*, Mexico, 2000, pp. 334–341

[28] C. Morris and H. Lecar, Voltage oscillations in the barnacle giant muscle fiber, *Biophysiological Journal* 35(1), (1981), pp. 193–213

[29] J. Nagumo, S. Arimoto and S. Yoshizawa, An active pulse transmission line simulating nerve axon, *Proc. IRE* 50, 1962, pp. 2061–2070.

[30] E. Neher and B. Sakmann, Single-channel currents recorded from membrane denervated frog muscle fibers, *Nature* 260, 1976, pp. 799–802.

[31] H. Nijmeijer and T. I. Fossen (eds.), *New Directions in Nonlinear Observer Design*, volume 244 of *Lecture Notes in Control and Information Science*, Springer-Verlag, London, 1999.

[32] C. M. A. Pinto and I. S. Labouriao, Two coupled neurons, in *IEEE International Conference on Computational Cybernetics (ICCC 2006)*, pp. 1–6.

[33] J. Reger, H. Sira Ramírez and M. Fliess, On non-asymptotic observation of nonlinear systems, in *Proc. of 44th IEEE Conference on Decision and Control*, Sevilla, Spain, 2000.

[34] J. Rinzel and G. B. Ermentrout, Methods in neuronal modeling, in C. Koch and I. Segev (eds.), *Methods in neuronal modeling*, chapter 7, MIT Press, Cambridge, MA, USA, 1989, pp. 135–169.

[35] K. Röbenack and A. F. Lynch, An efficient method for observer design with approximately linear error dynamics, *International Journal of Control* 77(7), 2004, pp. 607–612

[36] K. Röbenack, Direct approximation of observer error linearization for nonlinear forced systems, *IMA Journal of Mathematical Control and Information* 24(4), 2007, pp. 551–566.

[37] K. Röbenack, Residual generator based measurement of the current input into a cell, *Nonlinear Dynamics and Systems Theory* 9(4), 2009, pp. 425–434.

[38] K. Röbenack and P. Goel, Observer based measurement of the input current into a neuron, *Mediterranean Journal of Measurement and Control* 3(1), 2007, pp. 22–29.

[39] K. Röbenack and P. Goel, A combined observer and filter based approach for the determination of unknown parameters, *International Journal of Systems Science* 40(3), 2009, pp. 213–221.

[40] E. Rocha-Cózatl and J. Moreno, Passivity and unknown input observers for nonlinear systems, in *15th Triennial World Congress of the International Federation of Automatic Control Barcelona, 21-26 July 2002*.

[41] W. Sangtungtong, On Improvement in the Adaptive Sliding-Mode Speed Observer, *WSEA Transactions on Systems* 9(6), 2010, 581–593.

[42] Y. D. Sato and M. Shiino, Spiking neoron models with excitatory or inhibitory synaptic couplings and synchronization phenomena, *Physical Review E* 66, 2002, No. 041903.

[43] E. Schwartz (ed.), *Computational neuroscience*, MIT Press, Cambridge, Massachusetts, 1990.

[44] L. Shuang, W. Zhixin and W. Guoqiang, A Feedback Linearization Based Control Strategy for VSC-HVDC Transmission Converters, *WSEA Transactions on Systems* 10(2), 2011, 49–59.

[45] S. K. Spurgeon, Sliding mode obersers: a survey, *International Journal of Systems Science* 39(8), 2008, pp. 751–764.

[46] E. Steur, I. Tyukin and H. Nijmeijer, Semipassivity and synchronization of diffusively coupled neuronal oscillators, *Physica D: Nonlinear Phenomena* 238(21), 2009, pp. 2119–2128.

[47] R. E. Thomas and A. J. Rosa, *The Analysis and Design of Linear Circuits*, Wiley, 4th edition, 2004.

[48] R. D. Traub and R. Miles, *Neuronal networks of the hippocampus*, Cambridge University Press, Cambridge, 1991.

[49] R. D. Traub, J. G. R. Jefferys and M. A. Whittington, *Fast Oscillations in Cortical Circuits*, MIT Press, Cambridge, MA, 1999.

[50] S. Vassileva, V. Gantcheva and B. Tzvetkova, Inferential Measurement of gibberelline by predictive software analyzers, *Comptes rendus de l'Acaémie bulgare des Sciences (ISSN 1310-1331)* 63(9), 2010, 1359–1366.

[51] B. L. Walcott, M. J. Corless and S. H. Żak, Comparative study of non-linear state-observation techniques, *International Journal of Control* 45(6), 1987, pp. 2109–2132.

[52] S. Wu, Non-Linear Filtering in the Estimation of a Term Structure Model of Interest Rates, *WSEA Transactions on Systems* 9(7), 2010, 724–733.

[53] P. Young, Parameter estimation for continuous-time models a survey, *Automatica* 17(1), 1981, pp. 23–39.

[54] J. Zehetner, J. Reger and M. Horn, Echtzeit-Implementierung eines algebraischen Ableitungsschätzverfahrens, *Automatisierungstechnik* 55(11), 2007, pp. 553–560.